Experimental and theoretical spin configurations in Fe/Gd multilayers

M. Sajieddine, Ph. Bauer, K. Cherifi, C. Dufour, and G. Marchal
Laboratoire de Métallurgie Physique et Sciences des Matériaux, Université de Nancy I, Boîte Postale 239, F54506 Vandoeuvre-lès-Nancy Cedex, France

R. E. Camley
Department of Physics, University of Colorado, Colorado Springs, Colorado 80907
(Received 15 September 1993)

The experimental magnetic phase diagram for three characteristic Fe/Gd multilayered samples is confirmed on a microscopic scale by ^{57}Fe Mössbauer spectroscopy using a special geometry. The iron moment rotation in the sample plane at a critical H^* external field is observed and signals the transition from an aligned to a twisted state. This behavior is accounted for within the framework of an improved mean-field model. Self-consistent spin maps are derived for given temperatures and external fields applied parallel to the sample plane. A unique set of exchange coupling constants is used to calculate both the mean magnetic properties and the Mössbauer spectroscopy data.

I. INTRODUCTION

In the field of the magnetic properties related to iron/rare-earth multilayers, the theoretical study of the Fe/Gd system has become increasingly attractive for several reasons. Since Gd is in an S state, the magnetocrystalline anisotropy due to crystal-field effects is negligible when compared to other rare earths bearing an orbital moment. The very different ordering temperatures of Fe and Gd together with their antiparallel coupling at the interface give rise to complex and interesting magnetic phase diagrams as a function of layer thickness, temperature and external magnetic field.

Magnetic phase diagrams for Fe/Gd multilayers were first obtained theoretically by Camley and Tilley.[1,2] This work showed that when an external field was applied in the plane of the layers three main phases existed: (i) the Gd-aligned regime where gadolinium moments point in the field direction with iron moments in the opposite direction, (ii) the Fe-aligned regime where iron moments point in the field direction with gadolinium moments antiparallel, and (iii) the twisted regime where both iron and gadolinium moments leave the field direction and exhibit a transverse component. The Gd-aligned state occurs in a very low external field when the Gd magnetization overcomes the Fe one at low temperature. As the temperature increases, the Gd magnetization decreases and the net magnetization is nearly zero at a compensation temperature T_{cp}. Thus, for $T > T_{cp}$, the Fe-aligned state takes place. This state is found as well for samples with dominant iron magnetization at low temperature, i.e., when no compensation temperature exists. The twisted state sets in at a critical H^* field when a spin flop occurs, accompanied by a sudden increase of the susceptibility. Near T_{cp}, this transition takes place at a very low H^* field.

The theoretical predictions were consistent with the early work of Morishita, Togami, and Tsushima[3] who showed the occurrence of compensation temperatures and of Kamiguchi, Hayakawa, and Fujimori,[4] Fujimori, Kamiguchi, and Hayakawa[5] who evidenced spin flops through magnetoresistance effects. More recently, Cherifi and co-workers[6] established experimental phase diagrams for several Fex/Gdy samples with y/x close to two; the $H^*(T)$ curves were in qualitative accordance with the model. Furthermore, the transition between aligned and twisted states was evidenced on an atomic scale for a sample with dominant Gd magnetization at 100 K through ^{57}Fe Mössbauer spectroscopy by Bauer *et al.*[7] Using an original transmission geometry, these authors proved definitely the iron moment in-plane rotation with respect to an external field and derived the mean canting angle in the twisted state.

Direct fitting of the magnetic isotherms $M(H)$ was done first by Motokawa[8] for the Fe/Gd multilayered system by the use of a recursion formula which gave the angles between any magnetic moment and the field axis. More recently, fits of magnetization $M(H)$ and $M(T)$ curves as well as of magnetoresistance data for several Fex/Gdy samples with $x = y$ were reported by Takanashi *et al.*[9] within a self-consistent molecular field model. These authors assumed a stepwise modulation of the composition and the exchange interaction in Gd and Fe layers were the same as in bulk material. All these calculations led to theoretical H^* (spin flop) and T_{cp} (compensation temperature) in agreement with experimental data.

In this paper we report experimental data and theoretical calculations for the magnetic and ^{57}Fe Mössbauer properties of Fe/Gd multilayers with several compositions. Samples with dominant Gd magnetization at low temperature and samples with dominant Fe magnetization are examined. The model used originally in Ref. 1 is improved to take into account the actual layer thicknesses and the effective Gd magnetic moment at low field. The obtained spin configurations are used to calculate the $H^*(T)$ curves. The same spin maps allow us to account for both the transition probabilities of the ^{57}Fe nuclear Zeeman pattern and the evolution of the

0163-1829/94/49(13)/8815(6)/$06.00

hyperfine field versus the applied field H. The paper is organized as follows: Sec. II is devoted to experimental aspects, Sec. III recalls the model and its extensions, in Sec. IV we present the magnetic phase diagram, the Mössbauer spectroscopy results, and some characteristic calculated spin configurations for these Fe/Gd multilayers.

II. EXPERIMENT

Fe/Gd multilayered samples were obtained in a high-vacuum chamber by alternative deposition of iron and gadolinium on kapton foils kept at 90 K during the fabrication process. The pressure in the chamber was 10^{-9} Torr before the evaporation and 10^{-8} Torr during the process. To prevent contamination of the rare earth, the last layer was iron covered by silicon. Additional details of the fabrication are described in Ref. 10. The artificial periodic structure was confirmed by low-angle x-ray and low-angle neutron scattering. Because of the poor x-ray contrast between gadolinium and iron, the neutron technique was more appropriate despite the neutron absorption by Gd. A typical spectrum collected at room temperature on a Fe68 Å/Gd52 Å sample is pictured in Fig. 1. The modulations calculated from peak-to-peak distances were in accordance with expected ones within 6% accuracy. The crystallographic structure of the samples was examined by standard high-angle x-ray diffraction and *in situ* electrical measurements.[11] The Gd film becomes polycrystalline with hcp structure when the deposited layer is greater than 20 Å (grain size 35–55 Å). The structure of the Fe layers changes from amorphous to bcc when a critical thickness of 25 Å is reached. No preferred orientation was detected in the iron layers in the 30–60 Å thickness range, the iron layers are polycrystalline with an average grain dimension of 50 Å.

Magnetization measurements were done with a Foner-type magnetometer in fields up to 20 kOe and temperatures ranging from 4.2 to 300 K.[6] The field was applied parallel to the layers since the magnetization is thought to lie in the plane owing to dominant shape anisotropy.

Mössbauer spectra were recorded in transmission with standard source drive and data collection mode. The spectral analysis was carried out using Lorentzian line shapes. We recall that the line intensities of the ^{57}Fe nuclear Zeeman sextet depend on the angle θ between the Fe magnetization and the incident γ-ray beam. In the case of negligible quadrupole interaction, the absorption probability ratios for a thin absorber are expressed as $3{:}X{:}1$; $1{:}X{:}3$, where

$$X=4(1-\langle\cos^2\theta\rangle)/1+\langle\cos^2\theta\rangle\ .$$

For the studied Fe/Gd samples the usual setup (γ beam normal to the sample plane) yields $X=4$ indicating that the iron magnetization lies in the film plane as expected from demagnetizing field effects. When a magnetic field is applied parallel to the film planes, as was done for magnetization measurements, the value of X would obviously be kept at 4 whatever the in-plane moment orientation. Therefore, to obtain the variation of X versus the external field H, the sample was tilted around the H axis so that the sample normal made an angle of 45° with the γ beam. With this setup, one gets $X=4.00$ and $X=1.33$ for iron magnetic moments, respectively, parallel and perpendicular to the external field and $X=2.40$ for random orientation in the plane.[7]

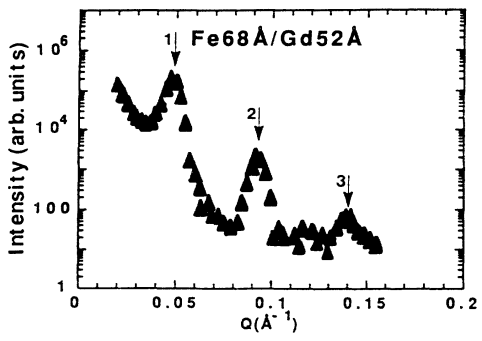

FIG. 1. Low-angle neutron-scattering pattern of a Fe68 Å/Gd52 Å multilayered sample showing three Bragg peaks representative of the periodic structure.

III. THE SELF-CONSISTENT MEAN-FIELD MODEL

A. Background

Theoretical calculations where done using a modified version of the original self-consistent mean-field model described in Ref. 1. The basic features may be summarized as follows. We consider alternative stackings of bcc iron and hcp gadolinium layers with an abrupt interface, despite the existence of slightly intermixed zones as revealed by Mössbauer spectroscopy. The spins are free to rotate in the atomic planes parallel to the interface planes and only nearest-neighbor interactions are considered. The exchange coupling constants are, respectively, J_1 for iron spins, J_2 for gadolinium spins, and J_I for antiferromagnetic coupling between iron and gadolinium spins at the interface. Inside a layer the Fe atom (resp. Gd atom) located in the ith monolayer has four (resp. three) nearest neighbors (nn) in monolayer $i+1$ and the same number in monolayer $i-1$. The spin in monolayer i is submitted to an effective field H_i which is the sum of the exchange field and the external field H:

$$H_i=\sum_{\text{nn}}(J_{i,i+1}\langle S_{i+1}\rangle+J_{i,i-1}\langle S_{i-1}\rangle)+H\ .$$

This spin is rotated in order to point in the direction of the effective field, so that the energy $E=-\Sigma_i H_i S_i$ is lowered. The thermal averaged magnitude $\langle S_i\rangle$ in that direction is given by the Brillouin function B: $\langle S_i\rangle=S_i B(S_i H/{}_i k_B T)$. The process is repeated until a self-consistent state is reached where all spins are aligned with the effective fields produced by the neighboring spins.

Different self-consistent states can be found depending on the initial choice for the spin configurations. For finite T and H the ground state corresponds to the lowest free energy $F=-k_B\ln(Z)-(\sum_i\langle S_i\rangle H)/2$ where Z is the partition function for the whole system and the second term on the right side eliminates the double

counting of the average exchange energy. In the mean-field approximation $Z=\Pi_i Z_i$ with Z_i being the partition function for the spin i in the self-consistent effective field. The output of this procedure consists of a spin map $S_{xi}^{\mathrm{Fe,Gd}}$, $S_{yi}^{\mathrm{Fe,Gd}}$ in the ith plane and from plane to plane along the perpendicular z direction within a period; the external field H is directed along the x axis. Following the layout of this spin map, the net magnetization along the external field direction H can thus be computed at each temperature T. For the fitting of microscopic data, the knowledge of S_{xi}^{Fe}, S_{yi}^{Fe} leads to $\sin^2\alpha_i$ where α_i is the angle between S_i and the applied field H. It is then possible, (i) to compute the $X(H)$ transmission ratio present in the ^{57}Fe Zeeman pattern through $\langle\cos^2\theta\rangle=\langle\sin^2\alpha\rangle/2$ and (ii) the resulting hyperfine field $H_{\mathrm{hyp}}(H)$; the latter is given by

$$(1/N_{\mathrm{Fe}})\Sigma_i[H_{\mathrm{hyp}}^2(0)+H^2-2H_{\mathrm{hyp}}(0)H\cos\alpha_i]^{1/2}\ ,$$

where N_{Fe} is the number of Fe monolayers within one period.

B. Choice of the parameters

The parameters used in the numerical analysis fall into two classes: (i) structural parameters related to the nominal thicknesses and the atom layer spacing and (ii) energy parameters and magnetic parameters which are adjustable to get the best fit but compatible with those corresponding to bulk material.

For the first kind we assume $[100]_{\mathrm{bcc}}\|[001]_{\mathrm{hcp}}$. If a and c are the lattice parameters of iron and gadolinium, the monolayer spacing is thus $a_{\mathrm{Fe}}=a/2$ and $a_{\mathrm{Gd}}=c/2$. From the individual layer thickness d_{Fe} and d_{Gd}, we get the number of monolayers within one period, i.e., $N_{\mathrm{Fe}}=d_{\mathrm{Fe}}/a_{\mathrm{Fe}}$ and $N_{\mathrm{Gd}}=d_{\mathrm{GD}}/a_{\mathrm{Gd}}$. In order to take care of the different densities in the stacking planes $(100)_{\mathrm{bcc}}$ and $(001)_{\mathrm{hcp}}$ at the interface, we write the ratio of total number of Fe and Gd atoms through the bulk densities and Avogadro number that is $n_{\mathrm{Fe}}/n_{\mathrm{Gd}}=1.4\ N_{\mathrm{Fe}}/N_{\mathrm{Gd}}$. It turns out that there are 1.4 times more Fe atoms per layer than Gd ones at the interface.

The second kind of parameters involves the exchange coupling constants J_1 between Fe atoms, J_2 between Gd atoms and J_I for antiparallel Fe-Gd coupling at the interface. An initial estimation of J_1 and J_2 is made from the bulk Curie temperature written as $T_C=J\ S(S+1)/3$. Here J, expressed in K, is a measure of the total effective exchange field acting on a spin, it includes in-plane contributions as well as contributions between planes. We assume furthermore these contributions to be equal, hence $J_1=J_{\mathrm{FE}}/3$ and $J_2=J_{\mathrm{Gd}}/3$. The antiparallel coupling exchange constant J_I should be negative and intermediate in absolute value between J_1 and J_2 as expected from data upon intermetallic Fe-Gd compounds.[12]

Calculations were at first performed with the hypothesis of bulk magnetic moments, i.e., $m_{\mathrm{Fe}}=2.2\mu_B$/atom and $m_{\mathrm{Gd}}=7.55\mu_B$/atom. The theoretical magnetic curves showed, however, that T_{cp} and H^* were larger than the experimental values and the $X(H)$ curves were shifted upward, indicating an excess of the gadolinium magnetization. Since it seemed unlikely to reduce d_{Gd} by 30%, we introduced further a phenomenological reduction of the total magnetic moment of the Gd films. In the present analysis, at variance with Takanashi *et al.*,[9] the iron magnetic moment was kept at $m_{\mathrm{Fe}}=2.2\mu_B$, consistently with the measured ^{57}Fe hyperfine field, but the "effective" gadolinium moment leading to good fits was found to fall around $m_{\mathrm{Gd}}=5.7\mu_B$, depending slightly upon the layer thickness. This assumption is supported experimentally: The saturation of a pure thin gadolinium probe was achieved only for fields above 20 kOe. This increased magnetic hardness may arise from the polycrystalline character of the Gd layers, more or less textured, and from possible defects. This statement being made for the gadolinium moment, the whole experimental data could be well accounted for with a unique set of energy parameters. Best fits were obtained with $J_1=521$, $J_2=16.5$, and $J_I=-200$ K. The parameter J_1 is consistent with the bulk Curie temperature of iron (1043 K), whereas J_2 led to a transition temperature of 260 K for gadolinium instead of 293 K.

IV. RESULTS AND DISCUSSION

Magnetization measurements, Mössbauer spectroscopy, and calculations were performed for various Fex/Gdy samples with or without compensation temperatures. We present results for three characteristic multilayers. Table I displays the compensation temperature, the structural parameters and the effective gadolinium moment which, for each sample, provides the best adjustments of the $M(H)$, $X(H)$, and $H_{\mathrm{hyp}}(H)$ curves.

As an example, we discuss the analysis performed on the Fe64 Å/Gd126 Å multilayer (sample II). Measurements of $M(H)$ are made at many different temperatures. At 4.2 K and for small applied fields the system is in the Gd-aligned state with the Gd moment parallel to the field

TABLE I. Compensation temperatures T_{cp} of selected Fex/Gdy samples together with their nominal thicknesses and related parameters: N_{Fe}, N_{GD} number of iron (gadolinium) monolayers in one stacking period. m_{Gd} is the effective gadolinium magnetic moment used for the calculations (see text). Sample III has dominant Fe magnetization at low temperature.

Sample No.	T_{cp} K	d_{Fe} (Å)	d_{Gd} (Å)	N_{Fe}	N_{Gd}	m_{Gd} (μ_B)
I	195	42	84	29	31	5.72
II	200	64	126	45	44	5.76
III		39	27	27	10	5.78

and the Fe moment antiparallel. In this phase the magnetization is nearly constant as a function of applied field. This low-susceptibility stage yields the Gd submagnetization and hence the effective reduced Gd moment $m_{Gd}=5.76\mu_B$, which we use throughout the calculations. As the external field is increased there is a phase transition to the twisted state at a particular field value H^*. This transition is marked by a significant increase in the magnetic susceptibility. If the field is kept constant and the temperature is increased the low susceptibility vanishes at the compensation temperature T_{cp} and then reappears above T_{cp} where the Fe magnetization dominates and points along the external field. The determination of H^* from several $M(H)$ isotherms leads to the experimental $H^*(T)$ curve which will be discussed below.

Two Mössbauer spectra recorded at 100 K for the same sample are displayed in Fig. 2. The spectrum 2(a) with $H=0$ kOe is analyzed with one subspectrum representative of bcc iron with the standard hyperfine field of 337 kOe and a hyperfine field distribution with a 10% depleted mean hyperfine field attributed to an interface where iron atoms feel the neighboring effects of gadolinium. The spectral abundance of this distribution leads to a mean interface thickness of 12 Å (6 Å on each side). The same analysis performed for the other samples shows that this interface does not depend upon the layer thickness itself for a constant substrate temperature during the deposition process. In the following we shall consider the evolution of the relative median lines depth $X(H)$ relevant to the main subspectra when an external field is applied. For instance in spectrum 2(b), the depth of these lines has clearly diminished at $H=3$ kOe, which signals an iron spin rotation in the sample plane.

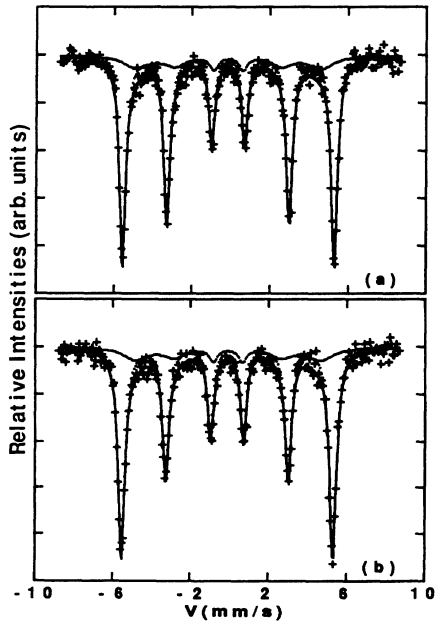

FIG. 2. Mössbauer spectra collected at 100 K in special transmission geometry for a Fe64 Å/Gd126 Å multilayer (sample II), $H=0$ kOe (a) and $H=3$ kOe (b). The minor component with broad lines is related to iron atoms involved in the interface.

A. Macroscopic magnetic properties

The experimental and calculated $H^*(T)$ curves for samples I-II-III are displayed in Fig. 3. The phase diagram illustrates the possible regimes. The borderline $H^*(T)$ separates the aligned and twisted states. For sample I and II the Gd-aligned state occurs for $T<T_{cp}$ and $H<H^*$ whereas the Fe-aligned state is stable when $T>T_{cp}$ and $H<H^*$. The calculated phase diagram $H^*(T)$ using the computed spin configurations is in accordance with the experimental one for the three samples: A minimum of H^* is found in the vicinity of T_{cp} separating the Gd-aligned and Fe-aligned states. As predicted theoretically, the H^* values are diminished when the layer thicknesses increase. Slight discrepancies occur however in the Fe-aligned state near room temperature, i.e., near the magnetic ordering point of gadolinium. In the case of sample III with dominant iron magnetization in the 4–300 K range, the overall behavior of $H^*(T)$ is about accounted for by the model but with the same limitations as for sample I and II near room temperature.

B. Mössbauer spectroscopy results

The results of the Mössbauer spectra analysis for samples I and II confirm the magnetic phase diagram $H^*(T)$

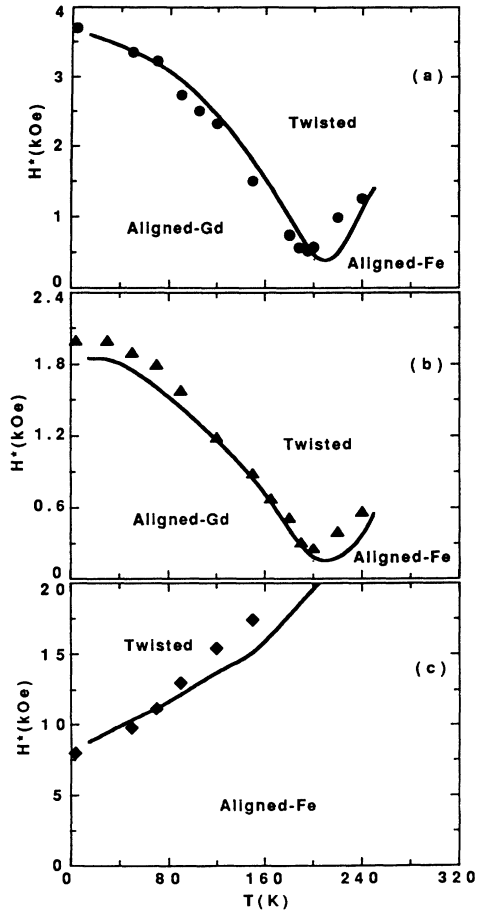

FIG. 3. Experimenal and theoretical magnetic phase diagram for (a) sample I (●), (b) II (▲), and (c) III (♦). The borderline $H^*(T)$ separates the aligned and twisted states (see text). The solid line represents calculated data.

on a microscopic scale. In Fig. 4 we display the evolution of the relative median line depth X and the total hyperfine field H_{hyp} versus the applied field H at three temperatures for sample I. The solid lines are calculated using the same theoretical spin configuration as above for the $H^*(T)$ curve. In the dominant Gd magnetization regime at $T=100$ K [Fig. 4(a)], X is close to 4 in remanent field ($H\approx 0$); near 2.5 kOe one observes a sudden decrease of X down to a minimum $X=1.5$ at $H=8.5$ kOe, then, X tends slowly towards 2.1 up to $H=13$ kOe. Going along with this evolution, H_{hyp} (H) is larger than $H_{hyp}(0)$ in the 0–8.5 kOe range and $H_{hyp}(H)$ is smaller than $H_{hyp}(0)$ in the 8.5–13 kOe range. This behavior can be interpreted as follows: At $H\approx 0$ the iron moments are almost antiparallel to the external field direction; at 2.5 kOe corresponding to H^*, they depart from this direction to come nearly perpendicular at $H=8.5$ kOe and as the external field is further increased they point more or less in the field direction. At 200 K, close to T_{cp}, the same evolution is seen in Fig. 4(b), but the drastic change in the iron moment orientation takes now place at a low H^* field (less than 1 kOe) and the minimum of $X(H)$ appears already at $H=2$ kOe. In the dominant iron magnetization regime at 240 K [Fig. 4(c)], a moment rotation still occurs at 1.5 kOe close to H^*, but there is no reversal with respect to the applied field this time since no maximum is to be found in the $H_{hyp}(H)$ curve.

The transition from the aligned states to the twisted state is also well demonstrated for sample II. However, the calculated $X(H)$ curve departs from experiment at low field. At 100 K in remanent field, the experimental $X(H)$ is far from 4 which would correspond to a strict alignment. The actual magnetic structure can no longer be considered as monodomain. Moreover at 250 K in the dominant iron magnetization regime, the transition Fe-aligned to twisted state is somewhat smeared out by possible domain rotation.

Finally Mössbauer spectra were taken at 100 K for sample III for which iron magnetization is always dominant. In the 1–13 kOe range, X is practically 4 whatever the field, meanwhile $H_{hyp}(H)$ decreases linearly indicating thus a steady Fe-aligned state (Fig. 5). Indeed, the transition to a twisted state cannot be detected here since H^*, close to 13 kOe, falls out of the available field range.

C. Spin maps

To illustrate the transition between aligned and twisted states we show in Fig. 6 some characteristic calculated spin maps for sample I. One and a half stacking periods are featured with $N_{Gd}=31$ and $N_{Fe}=29$ monolayers along the z axis, H is perpendicular to z. An arrow represents two layers and its length is proportional to the thermal averaged magnetic moment in that direction. Starting with the Gd-aligned state at 100 K for $H=2$ kOe in Fig. 6(a), all the Gd moments are parallel to the field direction and all the Fe moments antiparallel. At the interface, due to the neighboring effects of Fe, the Gd moment is enhanced with respect to its magnitude within the layer. At $H=4$ kOe, i.e., just above H^*, the twisted state is evidenced in Fig. 6(b): The Fe moments are slightly rotated and remain parallel to themselves. For that field, only one Gd moment is antiparallel to a Fe one at the interface, whereas the other Gd moments show a continuous rotation. Close to the compensation tempera-

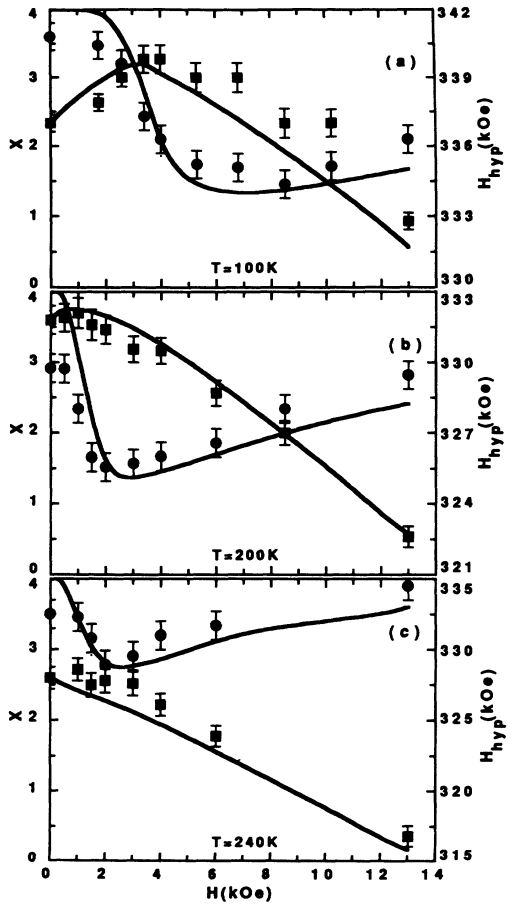

FIG. 4. Relative intensity X of the intermediate lines belonging to the main Zeeman pattern of the ^{57}Fe Mössbauer spectra (●) and hyperfine field $H_{hyp}(H)$ (■) versus the external magnetic field for sample I. $T=100$ K (a), $T=200$ K (b), and $T=240$ K (c). The solid lines represent calculated values.

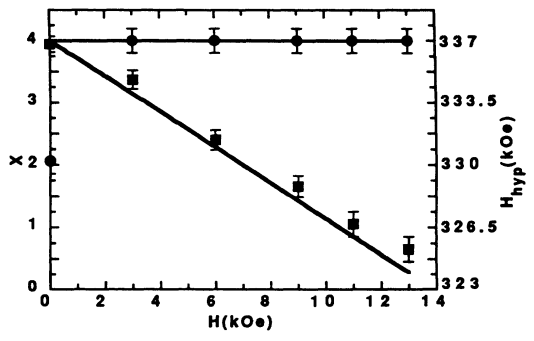

FIG. 5. Relative intensity X of the intermediate lines belonging to the main Zeeman pattern of the ^{57}Fe Mössbauer spectra (●) and hyperfine field $H_{hyp}(H)$ (■) versus the external magnetic field for sample III at $T=100$ K. The solid lines represent calculated values.

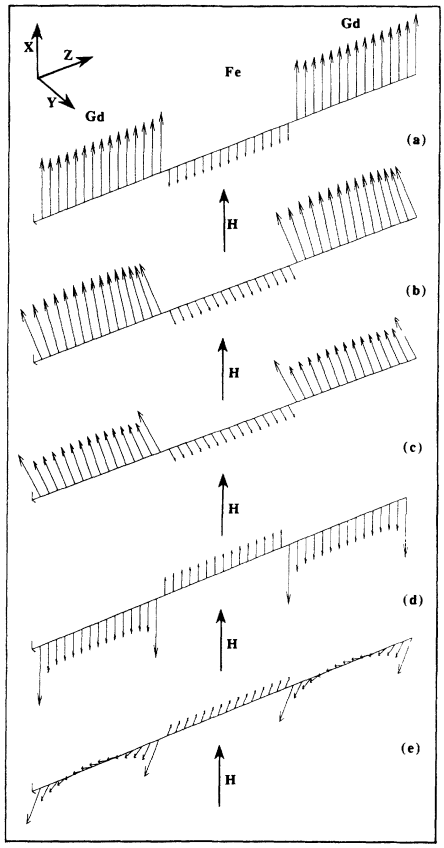

FIG. 6. Calculated spin maps for a Fe 42 Å/Gd 84 Å multilayer (sample I). From top to bottom: $T=100$ K with $H=2$ kOe (a) and $H=4$ kOe (b); $T=200$ K with $H=1.2$ kOe (c); $T=240$ K with $H=0.5$ kOe (d) and $H=1.5$ kOe (e).

ture T_{cp} [Fig. 6(c)], both Gd and Fe moments are nearly perpendicular to the field direction already at $H=1.2$ kOe, evidencing a low value of H^* at that temperature. At 240 K [Fig. 6(d)], when Fe magnetization overcomes that of Gd, the situation is reversed compared to Fig. 6(a): the Fe moments point in the field direction and the Gd ones oppositely for $H=0.5$ kOe. Just above H^*, at $H=1.5$ kOe [Fig. 6(e)], the iron moment rotation is less marked than the one observed for the gadolinium moments, which tend to point in the field direction when situated in the middle of the layer. All these features illustrate well the competition between the Zeeman and exchange energies; in particular, due to the relative low value of J_2 with respect to J_1 and $|J_I|$, the spread in the gadolinium moment orientation within one film is always more pronounced than that found in the Fe film.

V. CONCLUDING REMARKS

Two kinds of Fe/Gd nanoscale multilayers were synthesized by evaporation: samples with dominant Gd magnetization at low temperature and samples with dominant Fe magnetization at low temperature. Their magnetic phase diagram were determined experimentally using magnetic measurements. For all the samples the diagram is confirmed on a microscopic scale by ^{57}Fe Mössbauer spectroscopy using a special 45° geometry. The iron moment rotation in the sample plane at a critical H^* external field is observed and signals the transition from the aligned to the twisted state. This behavior is accounted for within the frame of a mean-field model. Self-consistent spin maps are derived for given temperatures and external fields applied parallel to the sample plane. A unique set of exchange-coupling constants is used to calculate the $H^*(T)$, $X(H)$, and $H_{hyp}(H)$ curves for a lot of samples in good agreement with experimental data. The exchange parameters J_1 (Fe-Fe) and J_2 (Gd-Gd) are consistent with those encountered for bulk material and, despite the lack of knowledge about the actual interface, the coupling between Fe and Gd is well accounted for by a parameter J_I negative and intermediate in absolute value with respect to J_1 and J_2. We had, however, to reduce the bulk magnetic moment of Gd to an effective moment; correlatively, the exchange coupling constant for Gd within a Gd layer was decreased by about 10%. A possible explanation lies in the polycrystalline character of these thin layers with enhanced magnetic hardness. Nevertheless, at the present stage, we think that the improved mean-field model where the actual stacking parameters have been properly taken into account, provides a realistic description of the magnetic properties and ^{57}Fe hyperfine interactions of the Fe/Gd multilayer system.

ACKNOWLEDGMENTS

The work of R.E.C. was supported by the U.S. ARO under Grant No. DAAL0391-G-0229 and by the University of Nancy. The Laboratoire de Métallurgie Physique et Sciences des Matériaux is Unité de Recherche Associée au CNRS No. 155.

[1]R. E. Camley and D. R. Tilley, Phys. Rev. B **37**, 3413 (1988).
[2]R. E. Camley, Phys. Rev. B **39**, 12 316 (1989).
[3]T. Morishita, Y. Togami, and K. Tsushima, J. Phys. Soc. Jpn. **54**, 37 (1985).
[4]Y. Kamiguchi, Y. Hayakawa, and H. Fujimori, Appl. Phys. Lett. **55**, 1918 (1989).
[5]H. Fujimori, Y. Kamiguchi, and H. Hayakawa, J. Appl. Phys. **67**, 5716 (1990).
[6]K. Cherifi, C. Dufour, Ph. Bauer, G. Marchal, and Ph. Mangin, Phys. Rev. B **44**, 7733 (1991); K. Cherifi, C. Dufour, G. Marchal, Ph. Mangin, and J. Hubsch, J. Magn. Magn. Mater. **104-107**, 1833 (1992).
[7]Ph. Bauer, M. Sajieddine, C. Dufour, K. Cherifi, G. Marchal, and Ph. Mangin, Europhys. Lett. **16**, 307 (1991).
[8]M. Motokawa, Prog. Theor. Phys., Suppl. **101**, 537 (1990).
[9]K. Takanashi, Y. Kamiguchi, H. Fujimori, and M. Motokawa J. Phys. Soc. Jpn. **61**, 3721 (1992).
[10]C. Dufour and G. Marchal, Rev. Sci. Instrum. **62**, 2984 (1991).
[11]C. Dufour, K. Cherifi, A. Bruson, G. Marchal, and Ph. Mangin, Phys. Status Solidi A **125**, 561 (1991).
[12]H. R. Kirchmayr and C. A. Poldy, J. Magn. Magn. Mater. **8**, 1 (1978).